

## Supporting Information

### **Selective oxidation of alcohols by graphene-like carbon with electrophilic oxygen and integrated pyridinic nitrogen active sites**

*Jiaquan Li,<sup>\*a</sup> Hongqi Sun,<sup>b</sup> Shaobin Wang,<sup>\*c</sup> Yu Dong<sup>d</sup> and Shaomin Liu<sup>a</sup>*

<sup>a</sup> WA School of Mines: Minerals, Energy and Chemical Engineering, Curtin University, Perth, WA 6102, Australia.

<sup>b</sup> School of Engineering, Edith Cowan University, Joondalup, WA 6027, Australia.

<sup>c</sup> School of Chemical Engineering and Advanced Materials, The University of Adelaide, Adelaide, SA 5005, Australia.

<sup>d</sup> School of Civil and Mechanical Engineering, Curtin University, Perth, WA, 6845, Australia.

Corresponding authors:

\* Jiaquan Li ([jiaquan.li@curtin.edu.au](mailto:jiaquan.li@curtin.edu.au))

\* Shaobin Wang. [shaobin.wang@adelaide.edu.au](mailto:shaobin.wang@adelaide.edu.au)

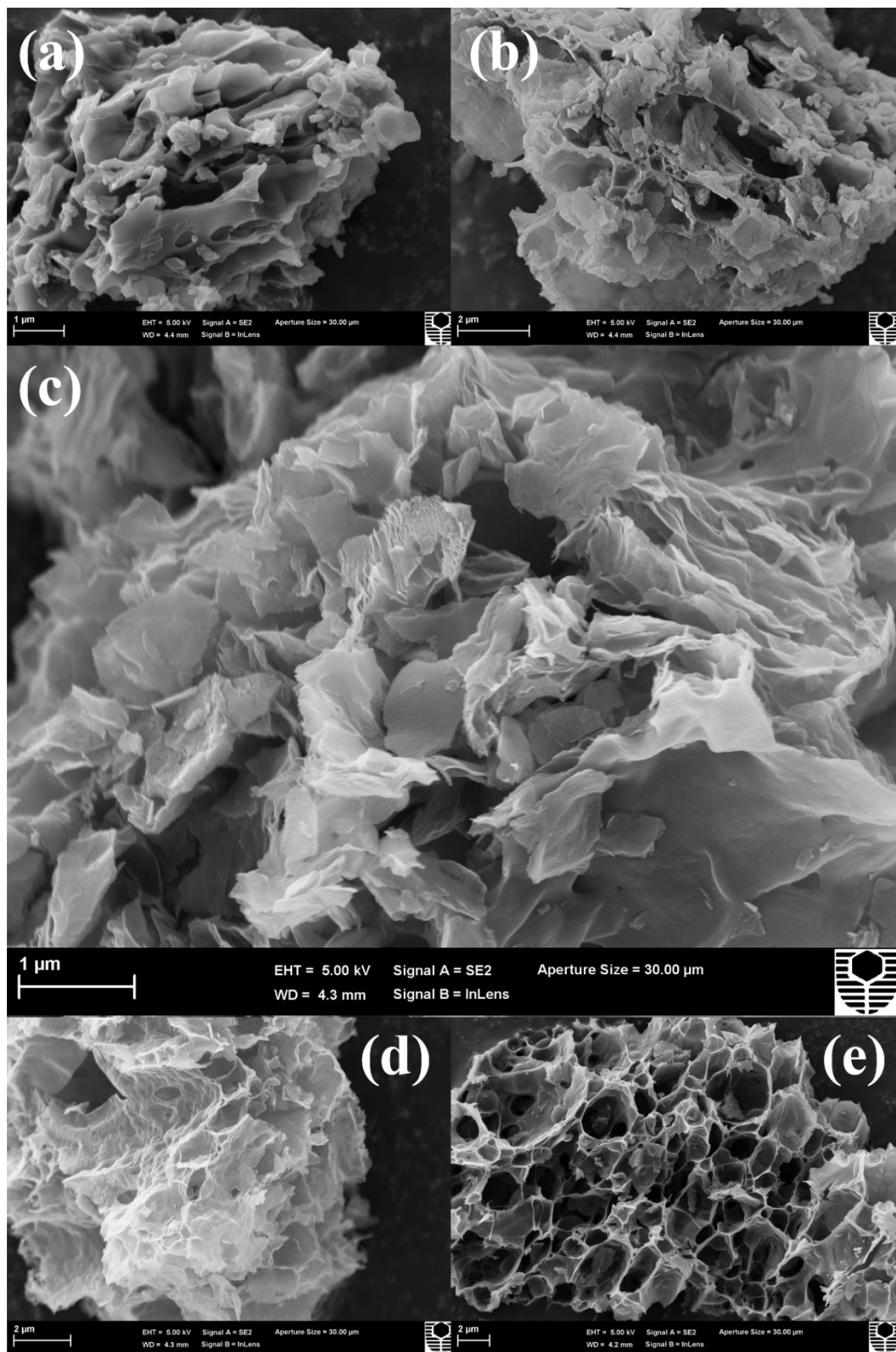


**Fig. S1.** SEM images of (a) NG-600, (b) NG-700, (c) NG-800, (d) NG-900 and (e) NG-1000.

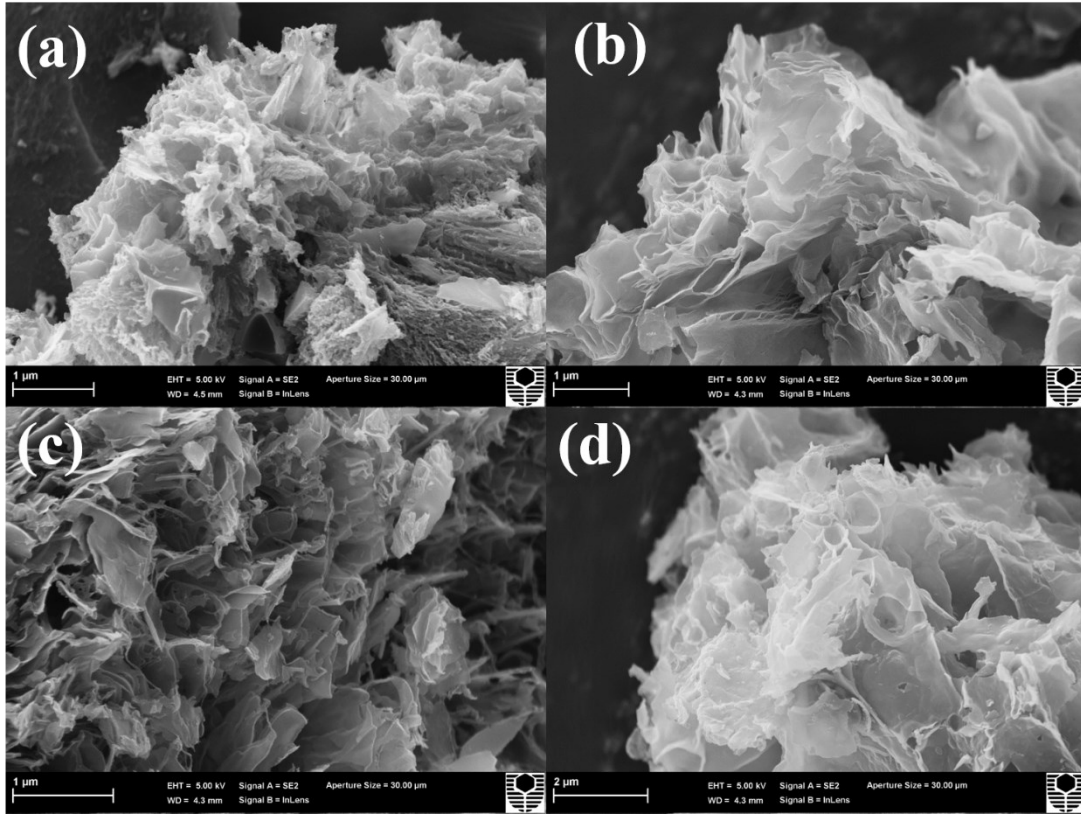


Fig. S2. SEM images of (a) NG(blank), (b) NG(AN), (c) NG(ACI) and (d) NG(MgN)

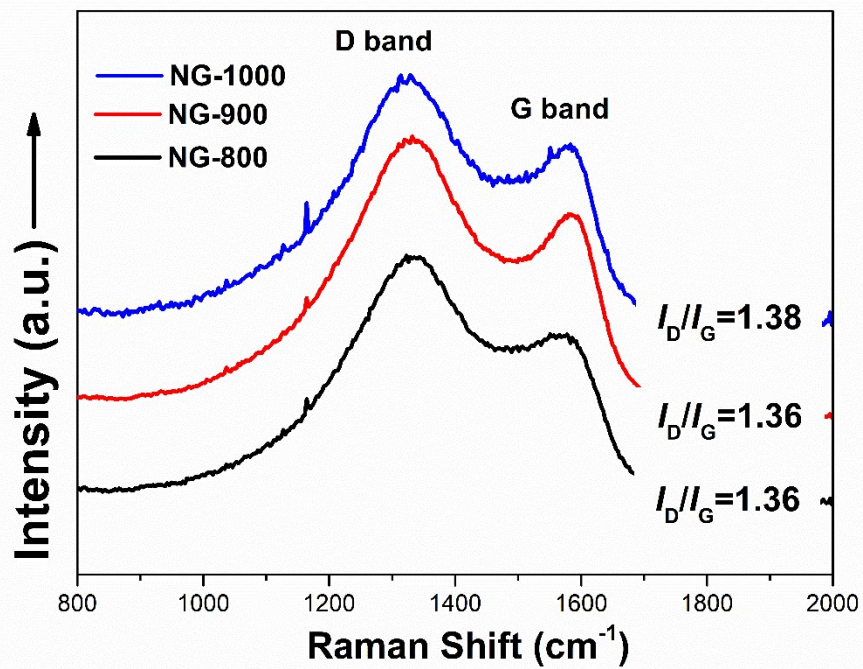
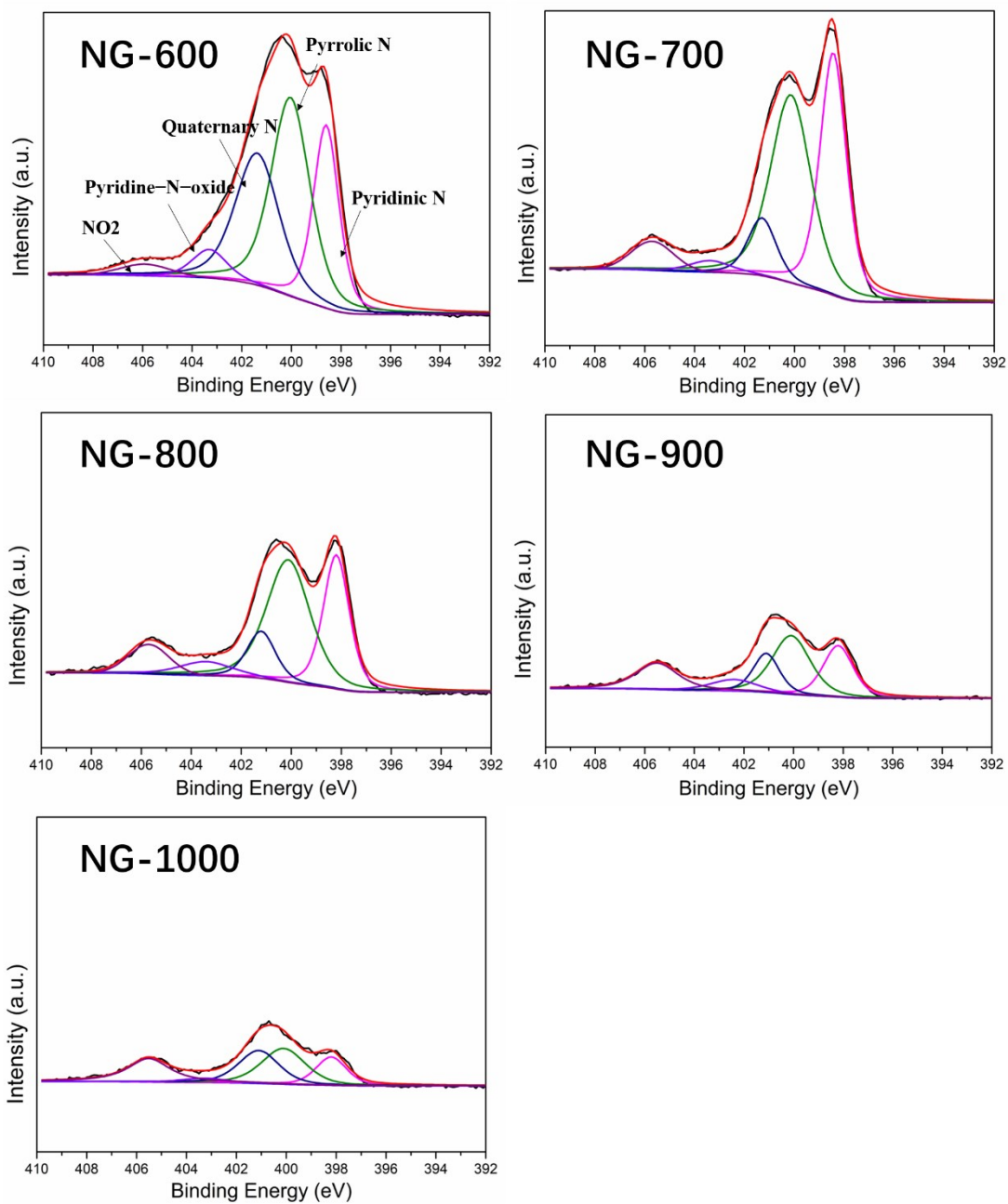
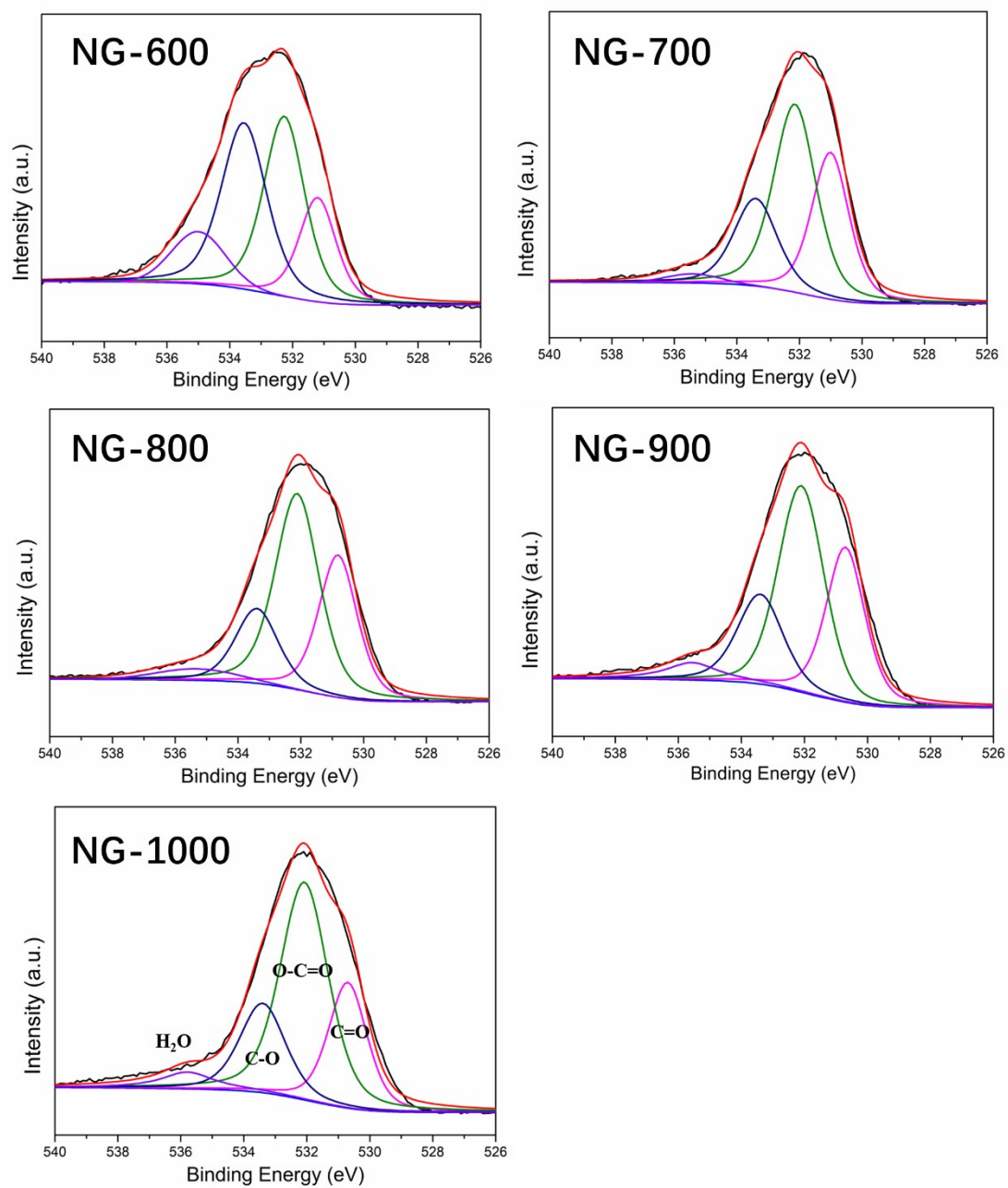


Fig. S3. Raman spectra of NG samples.



**Fig. S4.** Deconvolution of N1s XPS spectra of NG-600, NG-700, NG-800, NG-900 and NG-1000.



**Fig. S5.** Deconvolution of O1s XPS spectra of NG-600, NG-700, NG-800, NG-900 and NG-1000.

**Table S1.** Composition of O and N species on NG-600, NG-700, NG-800, NG-900 and NG-1000 derived from deconvolution of XPS spectra.<sup>a</sup>

Samples	Pyridinic N	Pyrolic N	Quaternary N	Pyridine-N-oxide	NO <sub>2</sub>	C=O	O=C-O	C-O	H <sub>2</sub> O
NG-600	5.5	9.1	6.9	1.2	0.6	1.7	3.2	3.3	1.0
NG-700	6.7	7.9	1.7	0.5	1.1	3.1	4.6	2.2	0.2
NG-800	3.6	5.6	1.4	0.8	1.0	2.8	4.4	1.6	0.4
NG-900	1.7	2.5	1.1	0.6	1.3	2.9	4.3	2.0	0.6
NG-1000	0.8	1.5	1.2	0.2	1.1	2.1	4.5	1.7	0.5

<sup>a</sup> The content of each N or O component is provided in atomic percentage.

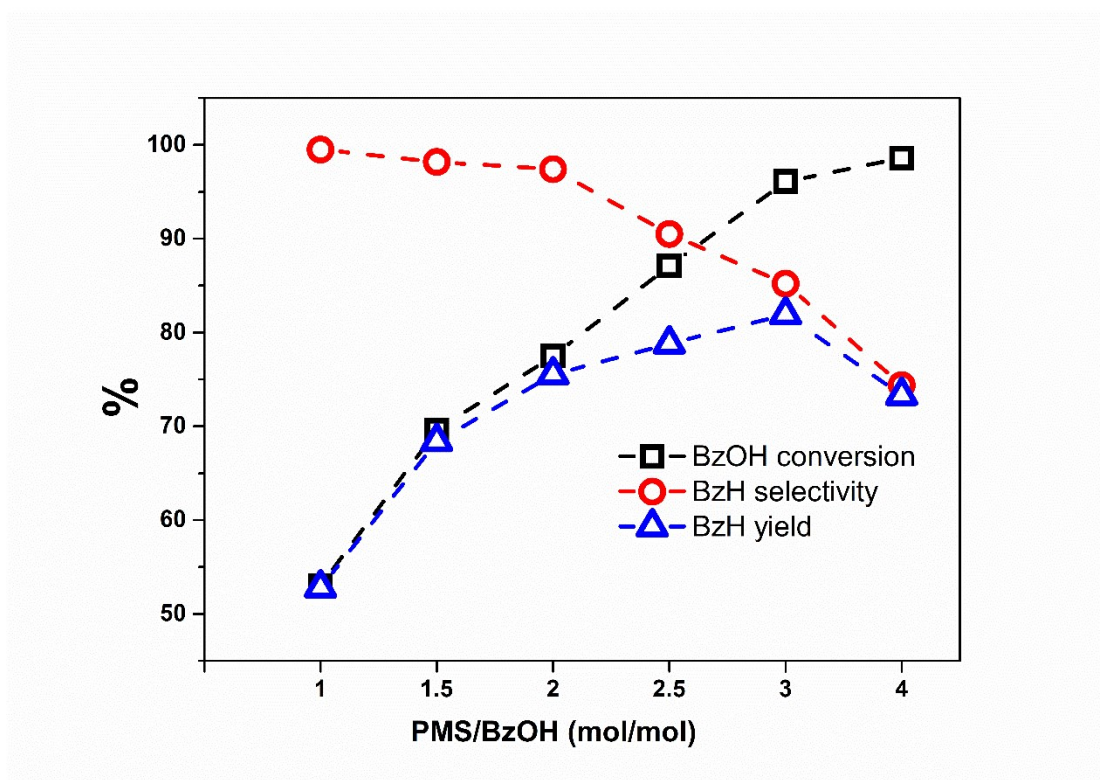


**Fig. S6.** The effect of PMS concentration on the catalytic efficiency of BzOH oxidation with NG-800. Reaction conditions: 5 mg catalyst, 0.1 mmol BzOH, 5 mL acetonitrile/water (1:1, volume ratio), 50 °C, 5 h.

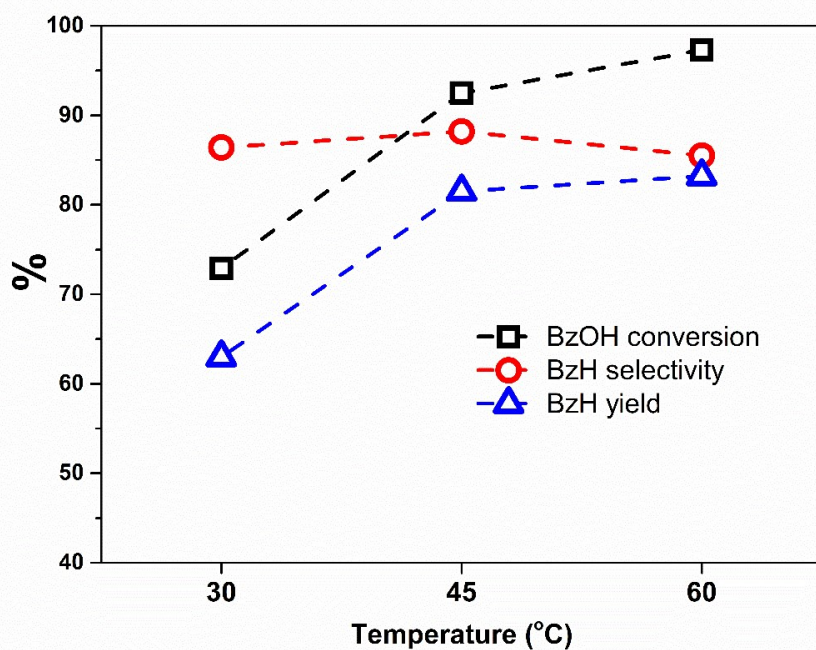


**Fig. S7.** The effect of reaction temperature on the catalytic efficiency of BzOH oxidation with NG-800. Reaction conditions: 5 mg catalyst, 0.1 mmol BzOH, 0.3 mmol PMS, 5 mL acetonitrile/water (1:1, volume ratio), 5 h.

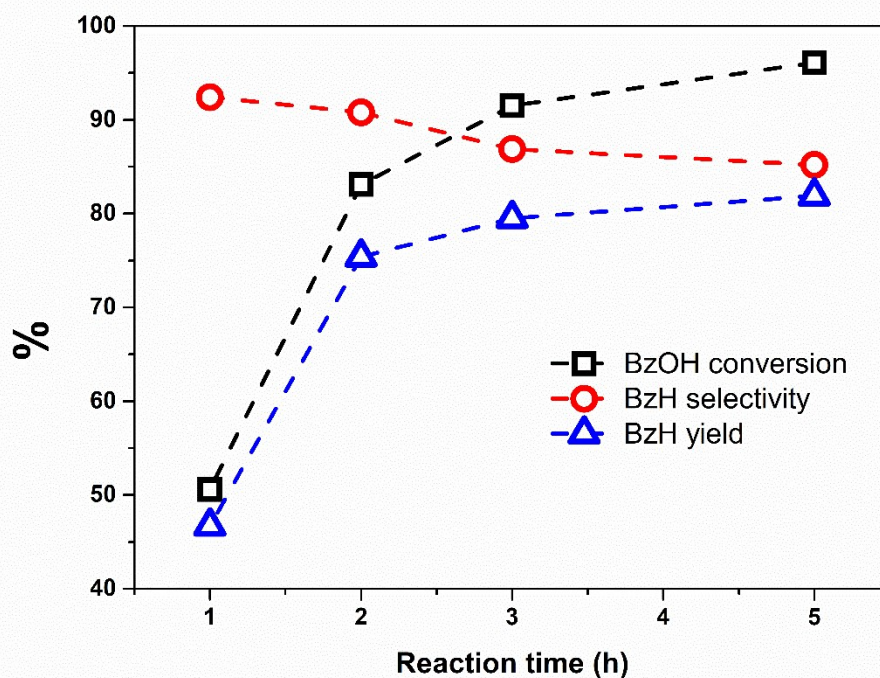


**Fig. S8.** The effect of reaction time on the catalytic efficiency of BzOH oxidation with NG-800. Reaction conditions: 5 mg catalyst, 0.1 mmol BzOH, 0.3 mmol PMS, 5 mL acetonitrile/water (1:1, volume ratio), 50 °C.

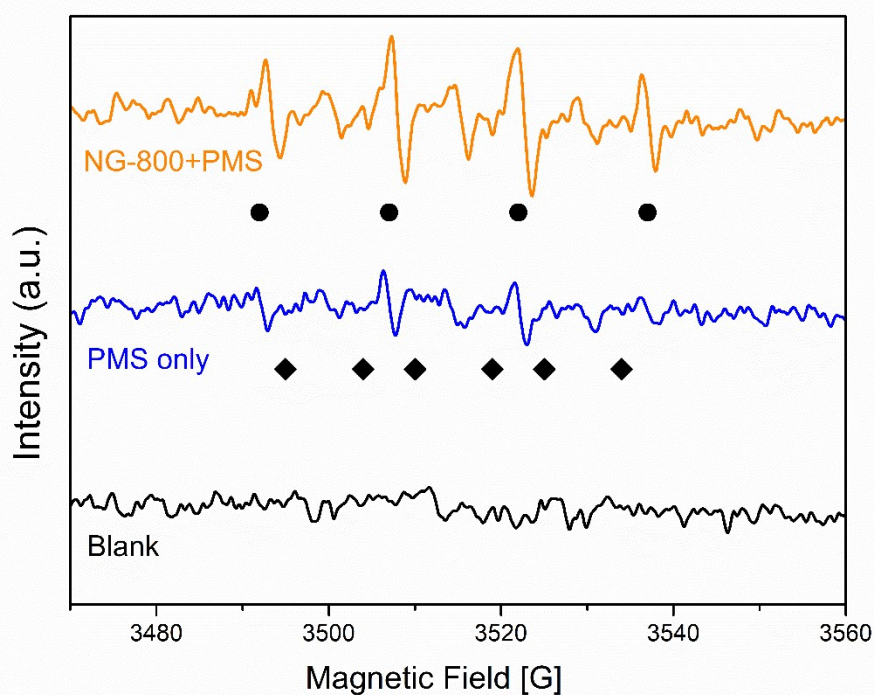


**Fig. S9.** EPR spectra in the presence of DMPO (DMPO- $\cdot$ OH- $\bullet$ , DMPO- $\text{SO}_4^{\cdot-}$ - $\blacklozenge$ ).

**Table S2.** Comparison of the oxidation efficiency of benzyl alcohol in this work with the reported literatures.

Entry	Catalyst loading (relative to the mass of BzOH)	Oxidant	T/°C	t/h	Additive	BzOH conversion/ %	BzH selectivity /%	BzH yield/%	Ref
1	Graphene oxide (200%)	O <sub>2</sub> /1 atm	100	24	–	–	–	90	[1]
2	NCNT (2%)	O <sub>2</sub> /15 atm	130	8	–	44.7	94.1	–	[2]
3	N-graphene (300%)	O <sub>2</sub> /1 atm	70	10	–	12.8	100	–	[3]
4	P-doped carbon (80%)	Air/1 atm	120	5	–	–	–	99.7	[4]
5	AuPd bimetal (0.5%)	O <sub>2</sub> /8 atm	110	1	–	83	70	–	[5]
6	NiFe <sub>2</sub> O <sub>4</sub> (10%)	TBHP	60	3	–	–	–	85	[6]
7	Au/Al <sub>2</sub> O <sub>3</sub> (2.5%)	TBHP	125	5	–	89.9	89.2	–	[7]
8	N-nanodiamond (5%)	TBHP	70	24	–	88.5	99	–	[8]
9	–	PMS	–	3	NaBr	–	–	87	[9]
10	Carbon nanotubes (50%)	PMS	50	5	–	57.1	84.3	48.1	[10]
11	NG (50%)	PMS	50	5	–	96.1	85.2	81.9	Herein



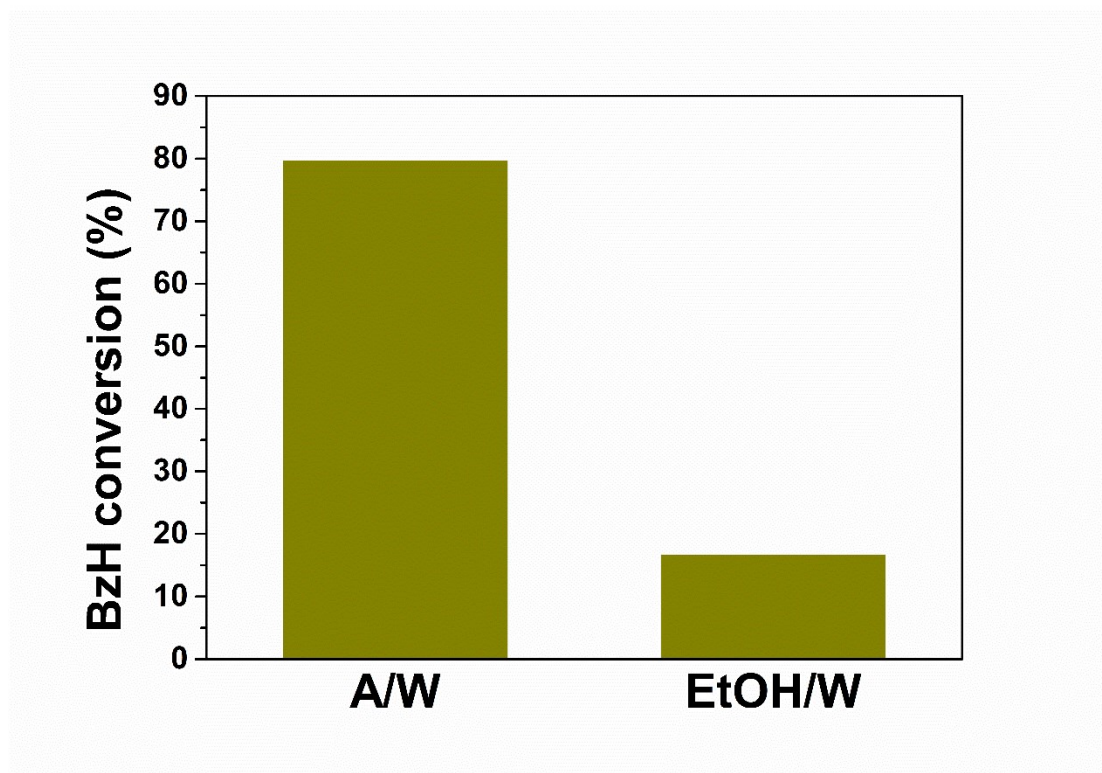


**Fig. S10.** The oxidation of BzH with NG-800 in acetonitrile/water 1:1 solvent (A/W) and ethanol/water 1:1 solvent (EtOH/W). Reaction conditions: 5 mg catalyst, 0.1 mmol BzH, 0.2 mmol PMS, 5 mL acetonitrile/water (1:1, volume ratio), 50 °C, 5 h.

## References

- [1] S. Presolski, M. Pumera, Graphene Oxide: Carbocatalyst or Reagent?, *Angew. Chem. Int. Ed.*, 57 (2018) 16713-16715.
- [2] J. Luo, H. Yu, H. Wang, H. Wang, F. Peng, Aerobic oxidation of benzyl alcohol to benzaldehyde catalyzed by carbon nanotubes without any promoter, *Chem. Eng. J.*, 240 (2014) 434-442.
- [3] J. Long, X. Xie, J. Xu, Q. Gu, L. Chen, X. Wang, Nitrogen-Doped Graphene Nanosheets as Metal-Free Catalysts for Aerobic Selective Oxidation of Benzylic Alcohols, *ACS Catal.*, 2 (2012) 622-631.
- [4] Z. Long, L. Sun, W. Zhu, G. Chen, X. Wang, W. Sun, P-Doped carbons derived from cellulose as highly efficient metal-free catalysts for aerobic oxidation of benzyl alcohol in water under an air atmosphere, *Chem. Commun.*, 54 (2018) 8991-8994.
- [5] P. Wu, Y. Cao, L. Zhao, Y. Wang, Z. He, W. Xing, P. Bai, S. Mintova, Z. Yan, Formation of PdO on Au-Pd bimetallic catalysts and the effect on benzyl alcohol oxidation, *J. Catal.*, 375 (2019) 32-43.
- [6] S. Iraqui, S.S. Kashyap, M.H. Rashid, NiFe<sub>2</sub>O<sub>4</sub> nanoparticles: an efficient and reusable catalyst for the selective oxidation of benzyl alcohol to benzaldehyde under mild conditions, *Nanoscale Advances*, 2 (2020) 5790-5802.
- [7] M.J. Ndolomingo, R. Meijboom, Selective liquid phase oxidation of benzyl alcohol to

benzaldehyde by tert-butyl hydroperoxide over  $\gamma$ -Al<sub>2</sub>O<sub>3</sub> supported copper and gold nanoparticles, *Appl. Surf. Sci.*, 398 (2017) 19-32.

[8] Y. Lin, Z. Liu, Y. Niu, B. Zhang, Q. Lu, S. Wu, G. Centi, S. Perathoner, S. Heumann, L. Yu, D.S. Su, Highly Efficient Metal-Free Nitrogen-Doped Nanocarbons with Unexpected Active Sites for Aerobic Catalytic Reactions, *ACS Nano*, 13 (2019) 13995-14004.

[9] B.-S. Koo, C.K. Lee, K.-J. Lee, OXIDATION OF BENZYL ALCOHOLS WITH OXONE® AND SODIUM BROMIDE, *Synth. Commun.*, 32 (2002) 2115-2123.

[10] J. Li, M. Li, H. Sun, Z. Ao, S. Wang, S. Liu, Understanding of the Oxidation Behavior of Benzyl Alcohol by Peroxymonosulfate via Carbon Nanotubes Activation, *ACS Catal.*, 10 (2020) 3516-3525.